Eur. Phys. J. C (2022) 82:675
https://doi.org/10.1140/epjc/s10052-022-10647-9

THE EUROPEAN PHYSICAL JOURNAL C

Regular Article - Theoretical Physics

Analytically approximation solution to Einstein-Cubic gravity

S. N. Sajadi[1,2,a], **S. H. Hendi**[1,2,3,b]

[1] Department of Physics, School of Science, Shiraz University, Shiraz 71454, Iran
[2] Biruni Observatory, School of Science, Shiraz University, Shiraz 71454, Iran
[3] Canadian Quantum Research Center, 204-3002 32 Ave, Vernon, BC V1T 2L7, Canada

Received: 12 April 2022 / Accepted: 26 July 2022

Abstract In this work, we introduce analytical approximate black hole solutions in Einstein-Cubic gravity. To obtain complete solutions, we construct the near horizon and asymptotic solutions as the first step. Then, the approximate analytic solutions are obtained through continued-fraction expansion. We also compute the thermodynamic quantities and use the first law and Smarr formula to obtain the analytic solutions for near horizon quantities. Finally, we follow the same approach to obtain the new static black hole solutions with different metric functions.

1 Introduction

Higher-order gravity models recently attracted considerable attention. In the context of cosmology, in order to go beyond the standard ΛCDM model and find an explanation for the late-time accelerated expansion, dark matter or inflation [1–4], higher-order curvature gravity theories are helpful. In AdS/CFT context, higher-order gravities have been used as tools to characterize numerous properties of strongly coupled conformal field theories [5–10]. From quantum gravity viewpoint, in order to unify quantum mechanics and gravitational interactions, going beyond the Einstein gravity is necessary [11].

In recent years, a new class of higher derivative theories has been discovered that is ghost-free and in four dimensions neither topological nor trivial known as Generalized Quasi-Topological Gravity [12–15]. One of the such higher-derivative gravity theories which in the four dimensions is neither topological nor trivial is Einsteinian cubic gravity. This theory of gravity, that has been recently proposed in [16], is the most general up to cubic order in curvature dimension independent theory of gravity that shares its graviton spectrum with Einstein's theory on constant curvature backgrounds. The Einsteinian cubic gravity field equations admit generalizations of the Schwarzschild solution, i.e. static, spherically symmetric solutions with a single metric function [17–19]. The Lagrangian density of this theory is given by [17,20]

$$L = R - 2\Lambda + \beta_1\kappa_4 + \beta_2\kappa_6 + \alpha P,$$

where κ_4 and κ_6 are four and six-dimensional Euler densities and correspond to the usual Lovelock terms, and P is the cubic term. In 4-dimensions the terms proportional to β_1 and β_2 have no contribution on the field equations. In [17–21], the authors construct static and spherically symmetric generalizations of the Schwarzschild and Reissner–Nordström-(Anti-)de Sitter black hole solutions in four-dimensions and study the orbit of massive test bodies near a black hole, especially computing the innermost stable circular orbit. They compute constraints on the ECG coupling parameter and the shadow of an ECG black hole. In [22], bounce universe in the critical point of the coupling constants of the theory has been studied. In [23], the holographic complexity of AdS black hole in Einsteinian cubic gravity has been investigated through the "complexity equals action" and "complexity equals volume" conjectures. In [24] the condensation of a charged scalar field in a (3 + 1)-dimensional asymptotically AdS background in the context of Einsteinian cubic gravity has been studied. In [25] holography on squashed-spheres, in [26] the holographic entanglement entropy, and in [27] various aspects of holographic ECG have been studied. In [20], the gravitational lensing due to the presence of supermassive black holes at the center of the Milky Way and other galaxies in Einsteinian Cubic Gravity has been studied.

In this paper, by using the continued fraction expansion technique, we obtain the static spherically symmetric solutions for the theory. This ansatz is designed so that the coefficients in the continued fraction are fixed by the behavior of the metric near the event horizon, while the pre-factors are introduced to match the asymptotic behavior at infinity [28–30].

[a] e-mail: naseh.sajadi@gmail.com (corresponding author)
[b] e-mail: hendi@shirazu.ac.ir

Published online: 05 August 2022

This method is an accurate analytic method that has recently been applied with success in a variety of contexts [31,32]. These analytic studies of the black hole also allowed us to study thermodynamics and other properties of the solutions. While, the numerical solutions do not give a clear picture of the metric dependence on physical parameters of the system.

The paper is organized as follows: in the next section, we first review Einsteinian cubic gravity and continued-fraction expansion. Then, calculating the thermodynamical quantities and inserting them in the first law and Smarr formula, we obtain the solutions for the near horizon quantities. We also plotted the metric functions and thermodynamical quantities and compared them with the previous works on this theory, we find a good agreement between them. In Sect. 3, we introduce new solutions of the theory with different metric functions. Finally, we conclude the paper in Sect. 4.

2 Basic equations

In 4D, Einstein cubic gravity theory is determined by the action [17–21]

$$\mathcal{S}=\frac{1}{16\pi G}\int d^4x\sqrt{-g}(R-2\Lambda+\alpha P-\kappa F_{ab}F^{ab}), \quad (1)$$

where R represent the Ricci scalar, α is coupling constant of the theory, and P cubic-in-curvature correction to the Einstein-Hilbert action is given as [17–21]

$$\begin{aligned}P=&12R_a{}^c{}_b{}^dR_c{}^e{}_d{}^fR_e{}^a{}_f{}^b+R_{ab}{}^{cd}R_{cd}{}^{ef}R_{ef}{}^{ab}\\&-12R_{abcd}R^{ac}R^{bd}+8R_a{}^bR_b{}^cR_c{}^a.\end{aligned} \quad (2)$$

The correction term in four dimensions is dynamical and is not topological or trivial [17–21]. Using the variational principle, one can find the following equation of motion

$$\begin{aligned}&E_{ab}=P_{acde}R_b{}^{cde}-\frac{1}{2}g_{ab}L-2\nabla^c\nabla^dP_{acdb}-2T_{ab}=0,\\&\nabla_aF^{ab}=0,\qquad T_{ab}=F_{da}F_b^d-\frac{1}{4}g_{ab}F_{de}F^{de}\end{aligned} \quad (3)$$

where L is the Lagrangian of Einstein cubic gravity and $P^{abcd}=\partial L/\partial R_{abcd}$ is

$$\begin{aligned}P_{abcd}=&g_{a[c}\,g_{b]d}+6\alpha\Big[R_{ad}R_{bc}-R_{ac}R_{bd}+g_{bd}R_a^eR_{ce}\\&-g_{ad}R_b^eR_{ce}-g_{bc}R_a^eR_{de}+g_{ac}R_b^eR_{de}\\&-g_{bd}R^{ef}R_{aecf}+g_{bc}R^{ef}R_{aedf}+g_{ad}R^{ef}R_{becf}\\&-3R_a{}^e{}_d{}^fR_{becf}\\&-g_{ac}R^{ef}R_{bedf}+3R_a{}^e{}_c{}^fR_{bedf}\\&+\frac{1}{2}R_{ab}{}^{ef}R_{cdef}\Big].\end{aligned} \quad (4)$$

Here, we consider the following spherically symmetric and static line element for describing the geometry of spacetime

$$ds^2=-f(r)dt^2+\frac{dr^2}{f(r)}+r^2\left(d\theta^2+\frac{\sin^2(\sqrt{k}\theta)}{k}d\phi^2\right). \quad (5)$$

As, we know generic static, spherically symmetric metrics do not need obey $g_{tt}g_{rr}=-1$ necessarily, but field equation (3) admits solutions with this property [17–21], to which case we shall restrict our consideration in this section.

By inserting the metric into the field equations, the differential equations for $f(r)$ become

$$\begin{aligned}E_r^r-2T_r^r=&\frac{1}{4r^5}[24\alpha r^2ff'''(2k-2f+rf')\\&+24\alpha r^3ff''^2+r(r^4+12\alpha rff'\\&-96k\alpha f+96\alpha f^2)f''\\&+24\alpha r(4f-k)f'^2+4r^3(-k+f+\Lambda r^2)\\&+(96k\alpha f+6r^4\\&-96\alpha f^2)f']+\frac{q^2}{r^4}=0.\end{aligned} \quad (6)$$

Expanding the function $f(r)$ around the event horizon r_+

$$f(r)=f_1(r-r_+)+f_2(r-r_+)^2+f_3(r-r_+)^3+... \quad (7)$$

and then inserting these expressions into Eq. (6), we find

$$\begin{aligned}f_2=&\frac{-2\Lambda r_+^4+2kr_+^2+12\alpha kf_1^2-3f_1r_+^2-2q^2}{r_+^4},\\f_3=&\frac{1}{3r_+^5+72\alpha r_+^3f_1^2+144\alpha r_+^2f_1k}\Big[-6f_2r_+^4\\&+f_1r_+^3(1-48\alpha f_2^2)+4r_+^2(24\alpha f_1^2f_2-k)\\&+48\alpha f_1r_+(-f_1^2+3kf_2)+8q^2-96\alpha kf_1^2\Big],\\f_4=&-\frac{1}{r_+^6(96\alpha f_1k+48\alpha r_+f_1^2+r_+^3)}\\&\times\Big[20q^2+144\alpha kf_2f_3r_+^3+48\alpha f_2^3r_+^4-384\alpha f_1f_2^3r_+^4\\&-384\alpha r_+^3f_1f_2^2+9r_+^5f_3-4r_+^4f_2-6kr_+^6-f_1r_+^3\\&-360\alpha kf_1^2+624\alpha r_+^2f_2f_1^2-576\alpha r_+^3f_1^2f_3\\&-240\alpha r_+f_1^3-792\alpha kr_+^2f_1f_3+504\alpha f_1f_2f_3r_+^4\\&+720\alpha r_+kf_1f_2-144\alpha r_+^2kf_2^2\Big]\end{aligned} \quad (8)$$

where r_+, f_1 are undetermined constants of integration. In the large r limit, we linearize the field equations about the

Schwarzschild background

$$f(r) = 1 - \frac{2M}{r} + \epsilon F(r), \tag{9}$$

where $F(r)$ should be calculated from the field equations. We linearize the differential equation by keeping terms only to order ϵ, and the resulting differential equation for $F(r)$ takes the form

$$F''' + \gamma(r)F'' + \eta(r)F' + \omega(r)F + g(r) = 0, \tag{10}$$

where

$$\gamma(r) = -\frac{96\alpha r^2 + 1152\alpha M^2 - 768\alpha Mr - 96k\alpha r^2 + r^6 + 192\alpha kMr}{48\alpha r(2M - r)(3M - r + kr)}, \tag{11}$$

$$\eta(r) = \frac{-16\alpha r^2 k + 416\alpha M^2 - 240\alpha Mr + 48\alpha kMr + 16\alpha r^2 - r^6}{8\alpha r^2(2M - r)(3M - r + kr)}, \tag{12}$$

$$\omega(r) = -\frac{288\alpha kMr - 576\alpha Mr + 1680\alpha M^2 + r^6}{12\alpha r^3(2M - r)(3M + kr - r)}, \tag{13}$$

$$g(r) = \frac{(k-1)r^7 - q^2r^5 - 288M\alpha r^2(k-1) + 120\alpha M^2 r(5k-14) + 2208\alpha M^3}{12\alpha r^4(2M - r)(3M - r + kr)}. \tag{14}$$

In the large r limit and $k = 1$, the homogenous equation reads

$$F''' + \frac{r^4}{144M\alpha}F'' + \frac{r^3}{24M\alpha}F' + \frac{r^2}{36M\alpha}F = 0. \tag{15}$$

This equation can be solved exactly in terms of hypergeom functions

$$\begin{aligned} F(r) = {} & c_1 \text{hypergeom}\left(\left[\frac{1}{5}\right], \left[\frac{3}{5}\right], -\frac{r^5}{720M\alpha}\right) \\ & + c_2 r^2 \text{hypergeom}\left(\left[\frac{3}{5}\right], \left[\frac{7}{5}\right], -\frac{r^5}{720M\alpha}\right) \\ & + c_3 r \text{hypergeom}\left(\left[\frac{2}{5}, 1\right], \left[\frac{4}{5}, \frac{6}{5}\right], -\frac{r^5}{720M\alpha}\right). \end{aligned} \tag{16}$$

In the large r, $F(r)$ decays super-exponentially and can be neglected. More relevant is the particular solution, which reads

$$f_p(r) = \sum_{n=2} \frac{F_n}{r^n} = \frac{F_2}{r^2} + \frac{F_3}{r^3} + ... \tag{17}$$

By inserting the above expansions into the field equations (10) and solving order by order, one can get

$$\begin{aligned} f_p(r) = {} & \frac{q^2}{r^2} + \frac{F_4}{r^4} - \frac{432\alpha M^2}{r^6} + \frac{64M\alpha(23M^2 + 18q^2)}{3r^7} \\ & - \frac{4656M^2q^2\alpha}{7r^8} + \frac{432M\alpha F_4}{r^9} \\ & - \frac{736M^2F_4\alpha}{r^{10}} - \frac{995328M^3\alpha^2}{5r^{11}} \\ & + \frac{3456M^2\alpha^2(1831M^2 + 576q^2)}{11r^{12}} + \mathcal{O}\left(\frac{1}{r^{13}}\right). \end{aligned} \tag{18}$$

For α goes to zero, one expects the metric returning to the RN. As a result F_4 should be zero. The solution at large r, thereby giving

$$\begin{aligned} f(r) \approx 1 & - \frac{2M}{r} + \frac{q^2}{r^2} - \frac{432\alpha M^2}{r^6} + \frac{64M\alpha(23M^2 + 18q^2)}{3r^7} \\ & - \frac{4656M^2q^2\alpha}{7r^8} - \frac{995328M^3\alpha^2}{5r^{11}} \\ & + \frac{3456M^2\alpha^2(1831M^2 + 576q^2)}{11r^{12}}. \end{aligned} \tag{19}$$

It should be noted, the other components of field equations give the same results for (7)–(18). We wish to obtain an approximate analytic solution (for $k = 1$) that is valid near the horizon and at large r. To this end we employ a continued fraction expansion [31], and write

$$f(r) = xA(x), \qquad x = 1 - \frac{r_+}{r} \tag{20}$$

with

$$\begin{aligned} A(x) = {} & 1 - \epsilon(1 - x) + (a_0 - \epsilon)(1 - x)^2 \\ & + \cfrac{a_1(1 - x)^3}{1 + \cfrac{a_2 x}{1 + \cfrac{a_3 x}{1 + \cfrac{a_4 x}{1 + ...}}}} \end{aligned} \tag{21}$$

where we truncate the continued fraction at order 4. By expanding (20) near the horizon ($x \to 0$) and the asymptotic region ($x \to 1$) we obtain

$$\epsilon = -\frac{F_1}{r_+} - 1, \quad a_0 = \frac{q^2}{r_+^2}, \quad a_1 = -1 - a_0 + 2\epsilon + r_+ f_1 \tag{22}$$

for the lowest order expansion coefficients, with the remaining a_i given in terms of (r_+, f_1); we provide these expressions in the Appendix A.

The result is an approximate analytic solution for metric functions everywhere outside the horizon. For a static space time we have a timelike Killing vector $\xi = \partial_t$ everywhere outside the horizon and so we obtain

$$T = \left.\frac{f^{'}(r)}{4\pi}\right|_{r_+} = \frac{f_1}{4\pi} = \frac{(1-2\epsilon+a_1+a_0)}{4\pi r_+} = \frac{1+\delta(r_+,q)}{4\pi r_+}. \tag{23}$$

Extreme charged black hole solutions exist if $f_1 = 0$ implying that $a_1 = 2\epsilon - a_0 - 1$. We compute the entropy as follows [33,34]

$$\begin{aligned} S &= -2\pi \int_{Horizon} d^2x\sqrt{\eta}\frac{\delta L}{\delta R_{abcd}}\epsilon_{ab}\epsilon_{cd} \\ &= \frac{A}{4}\left[1+6\alpha\left(\frac{f'^2}{r_+^2}+\frac{4f'}{r_+^3}\right)\right] \\ &= \frac{A}{4}\left[1+6\alpha\left(\frac{f_1^2}{r_+^2}+\frac{4f_1}{r_+^3}\right)\right] \\ &= \frac{A}{4}\left[1+\frac{6\alpha(1+\delta(r_+,q))}{r_+^4}[5+\delta(r_+,q)]\right]. \end{aligned} \tag{24}$$

We now consider the thermodynamics of these black hole solutions, whose basic equations are the first law and Smarr formula

$$dM = TdS + \phi dq, \tag{25}$$

$$M = 2TS + q\phi, \tag{26}$$

where there are no pressure/volume terms since we have set $\Lambda = 0$. From Eq. (26) we have

$$M = \frac{r_+^4 + 30\alpha + 66\alpha\delta(r_+,q) + 42\alpha\delta^2(r_+,q) + r_+^4\delta(r_+,q) + 6\alpha\delta^3(r_+,q) + 2q^2r_+^2}{2r_+^2}, \tag{27}$$

yielding the mass parameter as a function of the horizon radius. In the following, we show that the asymptotic behavior of the mass (27) is the same as the mass of the Schwarzschild black hole. So, one can interpret the mass (27), as ADM mass. We now impose the first law (25), which becomes

$$\frac{\partial M}{\partial r_+}dr_+ + \frac{\partial M}{\partial q}dq = T\frac{\partial S}{\partial r_+}dr_+ + T\frac{\partial S}{\partial q}dq + \phi dq \tag{28}$$

yielding

$$\begin{aligned} &\frac{\partial M}{\partial r_+} - T\frac{\partial S}{\partial r_+} = 0, \quad \Longrightarrow \\ &60\alpha + 132\alpha\delta(r_+,q) + 84\alpha\delta^2(r_+,q) \\ &+ 12\alpha\delta^3(r_+,a) + 2q^2r_+^2 - 48\alpha r_+\frac{\partial\delta(r_+,q)}{\partial r_+} \\ &- 60\alpha r_+\delta(r_+,q)\frac{\partial\delta(r_+,q)}{\partial r_+} - r_+^5\frac{\partial\delta(r_+,q)}{\partial r_+} \\ &- 12\alpha r_+\delta^2(r_+,q)\frac{\partial\delta(r_+,q)}{\partial r_+} = 0 \end{aligned} \tag{29}$$

and

$$\begin{aligned} &\frac{\partial M}{\partial q} - T\frac{\partial S}{\partial q} - \phi = 0, \quad \Longrightarrow \\ &48\alpha\frac{\partial\delta(r_+,q)}{\partial q} + 60\alpha\delta(r_+,q)\frac{\partial\delta(r_+,q)}{\partial q} + r_+^4\frac{\partial\delta(r_+,q)}{\partial q} \\ &+ 12\alpha\delta^2(r_+,q)\frac{\partial\delta(r_+,q)}{\partial q} + 2q^2r_+^2 = 0 \end{aligned} \tag{30}$$

as differential equations that must be satisfied by $\delta(r_+, q)$. From now, we consider the case $q = 0$. So, from Eq. (29) one can get

$$\begin{aligned} &r_+^4(1+\delta(r_+))^2 + 24\alpha(1+\delta(r_+))^3 \\ &+6\alpha(1+\delta(r_+))^4 + 4c_1r_+^4 = 0, \end{aligned} \tag{31}$$

by solving above equation one can obtain solutions for $\delta(r_+)$ as:

$$\begin{aligned} \delta^{1,2} = &-2 + \frac{\sqrt{2\mathcal{U}}}{12\sqrt{\alpha}\mathcal{Q}^{\frac{1}{6}}} \pm \\ &\frac{i\sqrt{2}}{\sqrt{\alpha}\mathcal{Q}^{\frac{1}{6}}\mathcal{U}^{\frac{1}{4}}}\sqrt{864\sqrt{2\mathcal{Q}}\alpha^{\frac{3}{2}} + \sqrt{\mathcal{U}}\mathcal{Q}^{\frac{2}{3}}r_+ + \sqrt{\mathcal{U}}(r_+^7 + 288c_1\alpha r_+^3 + \mathcal{Q}^{\frac{1}{3}}(4r_+^4 - 144\alpha)) - 36\sqrt{2\alpha\mathcal{Q}}r_+^4} \end{aligned} \tag{32}$$

$$\delta^{3,4} = -2 + \frac{\sqrt{2\mathcal{U}}}{12\sqrt{\alpha}\mathcal{Q}^{\frac{1}{6}}} \pm \frac{\sqrt{2}}{\sqrt{\alpha}\mathcal{Q}^{\frac{1}{6}}\mathcal{U}^{\frac{1}{4}}}\sqrt{864\sqrt{2\mathcal{Q}}\alpha^{\frac{3}{2}} - \sqrt{\mathcal{U}}\mathcal{Q}^{\frac{2}{3}}r_+ - \sqrt{\mathcal{U}}(r_+^7 + 288c_1\alpha r_+^3 + \mathcal{Q}^{\frac{1}{3}}(4r_+^4 - 144\alpha)) - 36\sqrt{2\alpha\mathcal{Q}}r_+^4} \tag{33}$$

where

$$\begin{aligned}
\mathcal{P} &= 36\sqrt{2\alpha c_1}\\
&\quad\sqrt{192c_1\alpha r_+^8 + 373248c_1\alpha^3 + 24\alpha r_+^8 - 9216\alpha^2 c_1^2 r_+^4 - 20736c_1\alpha^2 r_+^4}\\
\mathcal{Q} &= (-864c_1 r_+^4\alpha + 31104c_1\alpha^2 + r_+^8 + \mathcal{P})r_+\\
\mathcal{U} &= 72\alpha\mathcal{Q}^{\frac{1}{3}} - 2r_+^4\mathcal{Q}^{\frac{1}{3}} + \mathcal{Q}^{\frac{2}{3}}r_+ + 288r_+^3c_1\alpha + r_+^7.
\end{aligned} \tag{34}$$

Inserting (32)–(34) into the thermodynamical quantities and plotting them, one can arrive Figs. 1, 3 and 5. In Fig. 1, we have illustrated the temperature, entropy, and mass for different values of parameters. In these figures, the black and red solid lines correspond to the physical solutions, while the green and blue solid lines correspond to the non-physical black hole solutions. The physical solutions have positive temperatures and mass. In these figures, the behavior of the red solid lines is similar to the Schwarzschild black hole, and the behavior of the black solid lines is different from that of Schwarzschild black holes. In Fig. 1a, we observe that, unlike the Einstein gravity case, it no longer diverges for $r_+ \to 0$. Instead, there is a maximum value T_{max} that is reached at $r_{+,max}$.

In Fig. 1b, c, the behavior of entropy and mass in the large radii are similar to the Schwarzschild black hole and in the small radii, unlike the Einstein gravity case, diverge for $r_+ \to 0$. Different panels of Fig. 2, compare our black hole solutions (solid and long dashed lines) with those obtained in [17–19] (dashed and dotted lines). The solid and dashed lines are the results of our calculus and the paper [17–19] for positive α, respectively. The long dashed and dotted lines are the results of our calculus and the paper [17–19] for negative α, respectively. As can be seen, there is a good agreement in both cases between our computations and the results of the mentioned papers in large radii and somewhat different in small radii but have the same behavior. This shows that the first law of thermodynamic and the Smarr formula in the form of (25) and (26) are valid for this theory of gravity.

In the following, we are going to look at the thermodynamical stability of the solutions. In global stability, we allow a system in equilibrium with a thermodynamic reservoir to exchange energy with the reservoir. The preferred phase of the system is the one that minimizes the free energy. In order to investigate the global stability, we use the following expression for the free energy

$$F = M - TS. \tag{35}$$

In Fig. 3a, we have shown the free energy in terms of r_+ for positive α. As can be seen in the black, green, and blue branches the free energy is decreasing functions of r_+. This shows the black holes in these branches globally are stable. While in the red branch, the free energy has an increasing behavior and is a globally unstable branch.

On the other hand, local stability is concerned with how the system responds to small changes in its thermodynamic parameters. In order to study the thermodynamic stability of the black holes with respect to small variations of the thermodynamic coordinates, one can investigate the behavior of the heat capacity. The positivity of the heat capacity ensures local stability. The heat capacity is given by

$$C = \frac{\partial M}{\partial T}. \tag{36}$$

In Fig. 3b, heat capacity in terms of r_+ for positive α have been illustrated. As can be seen the heat capacity in all radii is negative, this shows the black hole in all branches locally unstable.

In Fig. 4, the heat capacity and free energy are compared based on our calculations and the results of papers [17,18]. As can be seen from the dashed lines of both figures, the black holes in small radii are locally stable but globally unstable (Figs. 5, 6, 7).

In panels of Fig. 8, we have depicted the metric functions. In Fig. 8a and b, the mass of the black hole is positive and these solutions are similar to Schwarzschild's black hole. In Fig. 8c and d, the mass of black holes are negative and their behavior is different from the Schwarzschild black hole.

3 New solutions

Here, in order to obtain the new static, spherically symmetric black hole solutions of theory we consider a line element with different metric functions. We consider the following static metric

$$ds^2 = -h(r)dt^2 + \frac{dr^2}{f(r)} + r^2\left(d\theta^2 + \sin^2(\theta)d\phi^2\right). \tag{37}$$

Unlike the previous section, here we have two metric functions that require two components of field equations to obtain them. By inserting the metric into the field equations, the dif-

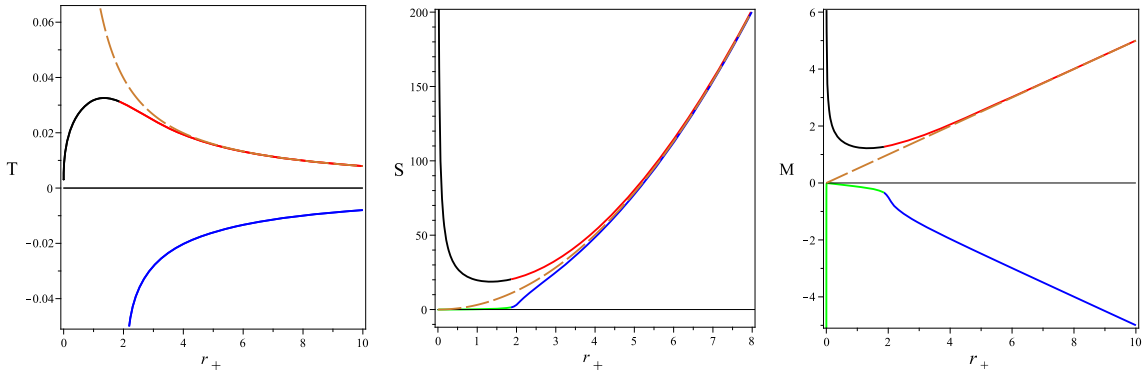

Fig. 1 The temperature, entropy and mass as a function of r_+ for $c_1 = -0.25, \alpha = 0.5$. The orange long dashed lines related to the Schwarzschild's black hole

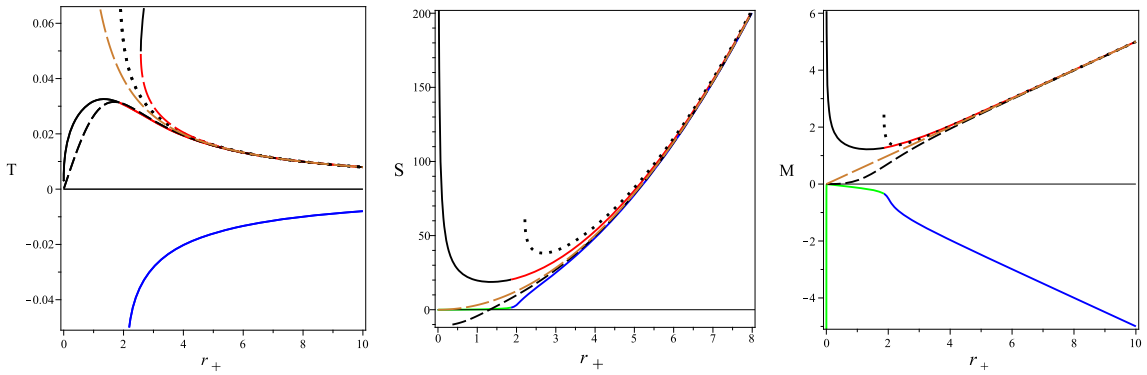

Fig. 2 The temperature, entropy and mass as a function of r_+ for $c_1 = -0.25, \alpha = 0.5$: solid lines are the results of our method and dashed lines are the results of the paper [17,18]. For $\alpha = -0.5$: Long dashed lines are the results of our method and dotted lines are for the paper [17,18]. The orange long dashed lines related to the Schwarzschild's black hole

Fig. 3 The free energy and heat capacity as a function of r_+ for $c_1 = -0.25, \alpha = 0.5$. The orange long dashed lines related to the Schwarzschild's black hole

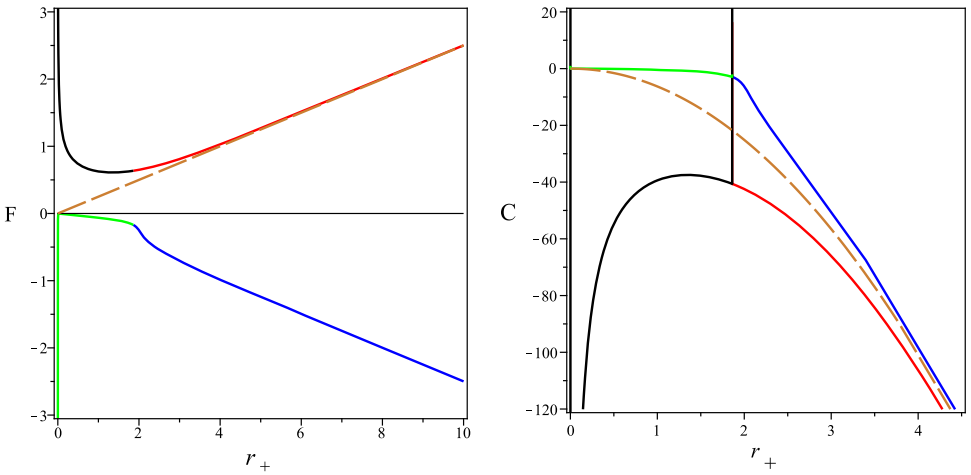

ferential equations for $f(r)$ and $h(r)$ become

$$
\begin{aligned}
8r^4h^4E_r^r = {} & h^3r^4f'h' + 4h^4r^3f' + 8r^2fh^4 \\
& + 8r^3h^3fh' + 2r^4fh^3h'' - h^2r^4fh'^2 - 8r^2h^4 - \\
& \alpha[-12r^2h^3h'f'^3 - 48rfh^3f'h'' \\
& + 24rhf^2h'^3 - 24rh^3h'f'^2 - 48rf^2h^2h'h'' + \\
& 24rf^2h^2f'h'^2 + 24fr^2h^2h'^2f'^2 \\
& - 24rhf^3h'^3 - 24r^2fh^3f'^2h'' - 48f^2h^3h'f' \\
& + 48rf^2h^3f'h'' + 48rf^3h^2h'h'' \\
& + 12r^2f^3h'^4 + 48fh^3h'f' \\
& + 24r^2f^2h^2f'h'h'' \\
& + 48rfh^3h'f'^2 - 24r^2hf^2f'h'^3
\end{aligned}
$$

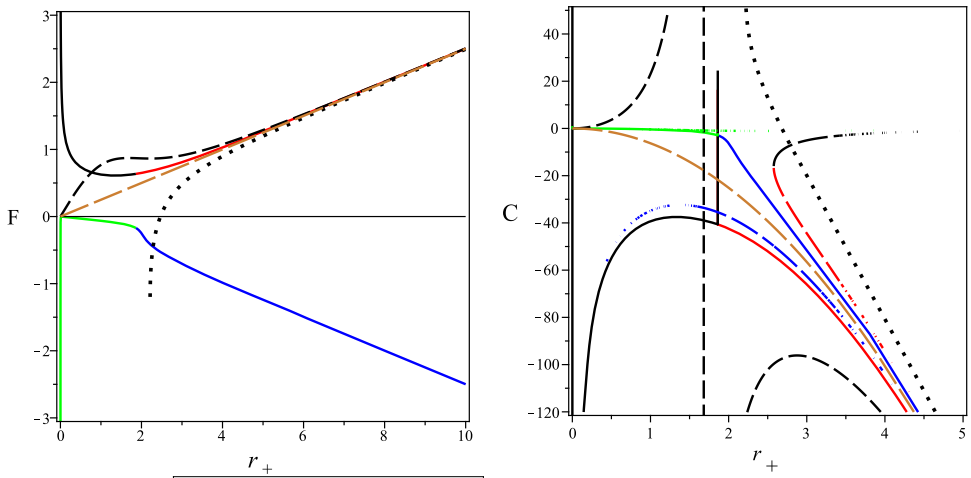

Fig. 4 The free energy and heat capacity as a function of r_+ for $c_1 = -0.25, \alpha = 0.5$: solid lines are the results of our method and dashed lines are the results of the paper [17,18]. For $\alpha = -0.5$: Long dashed lines are the results of our method and dotted lines are for the paper [17,18]. The orange long dashed lines related to the Schwarzschild's black hole

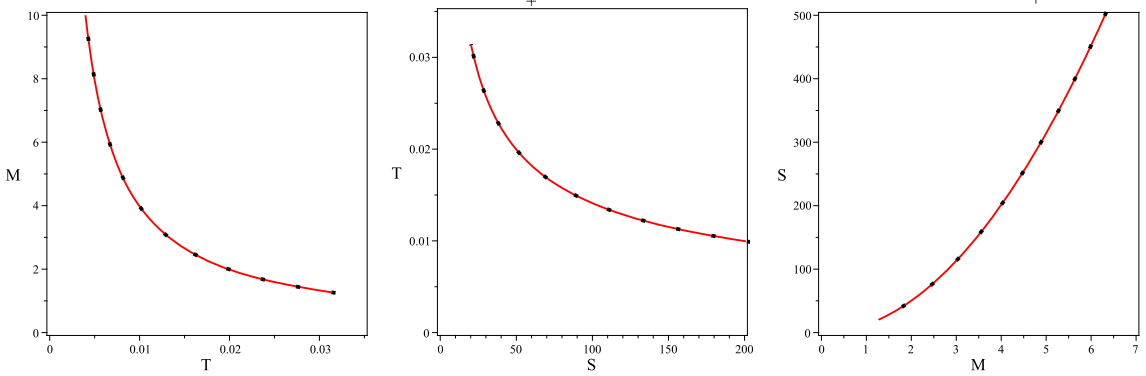

Fig. 5 The plots of temperature, entropy and mass for $c_1 = -0.25, \alpha = 0.5$

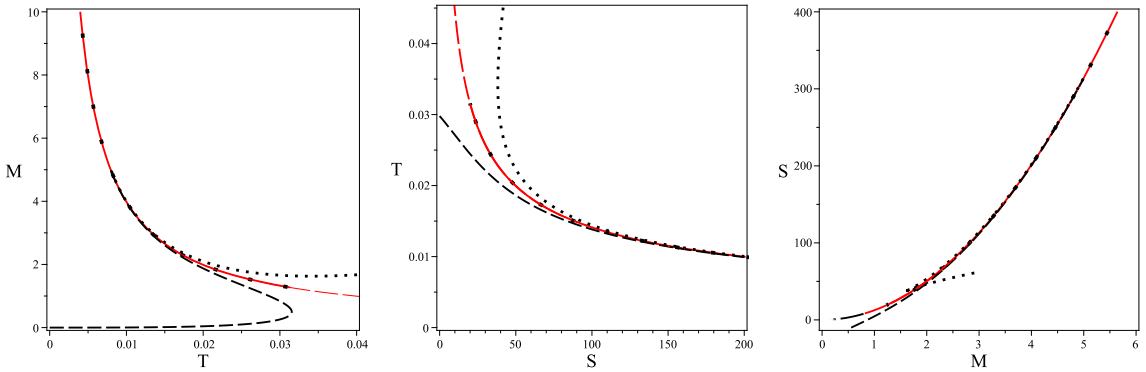

Fig. 6 The temperature, entropy and mass as a function of r_+ for $c_1 = -0.25, \alpha = 0.5$: solid lines are the results of our method and dashed lines are the results of the paper [17,18]. For $\alpha = -0.5$: Long dashed lines are the results of our method and dotted lines are for the paper [17,18]

$$- 24r^2 f^3 h h'^2 h''], \tag{38}$$

and

$$\begin{aligned}
-4r^4h^4E_a^a = &-3r^4h^3f'h' - 6r^4h^3fh'' - 12r^3h^4f' \\
&- 12r^2fh^4 - 12fr^3h^3h' + 3r^4fh^2h'^2 + 12r^2h^4 \\
&+ 3\alpha[-16r^2fh^3f'^2h'' + 32rf^2h^3f'h'' \\
&+ 32rfh^3h'f'^2 - 16r^2hf^2f'h'^3 \\
&- 16r^2hf^3h''h'^2 \\
&+ 16rf^2h^2f'h'^2 + 16r^2f^2h^2f'h'h'' \\
&+ 16r^2fh^2f'^2h'^2 - 8r^2h^3h'f'^3 \\
&+ 8r^2f^3h'^4 - 16rhf^3h'^3 \\
&+ 32rh^2f^3h'h'' - 32f^2h^3h'f' \\
&- 32rf^2h^2h'h'' - 32rfh^3f'h'' \\
&+ 16rhf^2h'^3 - 16rh^3f'^2h' \\
&+ 32fh^3h'f'].
\end{aligned} \tag{39}$$

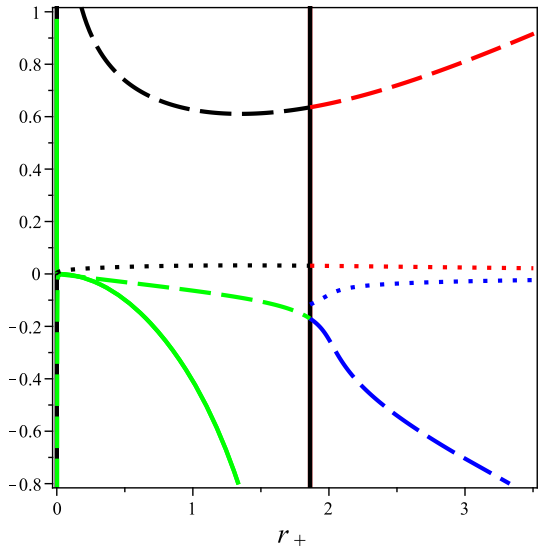

Fig. 7 The temperature (dotted line), heat capacity (solid line) and free energy (dashed line) as a function of r_+ for $c_1 = -0.25$, $\alpha = 0.5$

Similar to the previous section, expanding the function $h(r)$ and $f(r)$ around the event horizon r_+

$$f(r) = f_1(r - r_+) + f_2(r - r_+)^2 + f_3(r - r_+)^3 + ... \tag{40}$$

$$h(r) = h_1(r - r_+) + h_2(r - r_+)^2 + h_3(r - r_+)^3 + ... \tag{41}$$

and then inserting these expressions into the field equations, we find

$$f_2 = \frac{h_1 r_+^2 - h_1 f_1 r_+^3 + 6\alpha f_1^3 h_2 r_+^2 + 6\alpha h_1 f_1^2 + 12\alpha r_+ h_2 f_1^2}{6\alpha r_+ f_1 h_1 (2 + r_+ f_1)}, \tag{42}$$

where r_+, f_1, h_1 and h_2 are undetermined constants of integration. The other near horizon constants provided in the Appendix B. In the large r limit, we linearize the field equations near the Schwarzschild background

$$f(r) = 1 - \frac{2M}{r} + \epsilon F(r), \tag{43}$$

$$h(r) = 1 - \frac{2M}{r} + \epsilon H(r), \tag{44}$$

where $F(r)$ and $H(r)$ are determined by the field equations, and we linearize the differential equations by keeping terms only to order ϵ. The resulting differential equations for $F(r)$ and $H(r)$ take the form

$$H'' + \gamma(r)H' + \eta(r)F' + \omega(r)F(r) + \Xi(r)H(r) + g(r) = 0, \tag{45}$$

$$H'' + \bar{\gamma}(r)H' + \bar{\eta}(r)F' + \bar{\omega}(r)F(r) + \bar{\Xi}(r)H(r) + \bar{g}(r) = 0, \tag{46}$$

where the functions shown in the above equations are given in the Appendix C. In the large r limit, the homogenous equations read

$$H'' + \frac{4}{r}H' + \frac{2}{r}F' + \frac{4F}{r^2} - \frac{4MH}{r^3} = 0, \tag{47}$$

$$H'' + \frac{2}{r}H' + \frac{2}{r}F' + \frac{2F}{r^2} + \frac{2M^2H}{r^4} = 0. \tag{48}$$

Equations (47) and (48) can be solved exactly to obtain

$$F(r) = \frac{M}{\sqrt{\pi} r^2}\left[2c_2' r e^{-\frac{(M+2r)^2}{r^2}} + \sqrt{\pi}(M + 2r)\left(c_1' + c_2' erf\left(2 + \frac{M}{r}\right)\right)\right], \tag{49}$$

$$H(r) = c_1 + c_2 erf\left(2 + \frac{M}{r}\right). \tag{50}$$

In the large r, $F(r)$ and $H(r)$ become

$$F(r) \approx \frac{2M(\sqrt{\pi}c_1' + \sqrt{\pi}c_2' erf(2) + c_2' e^{-4})}{\sqrt{\pi} r} + \frac{M^2(\sqrt{\pi}c_1' + \sqrt{\pi}c_2' erf(2) - c_2' e^{-4})}{\sqrt{\pi} r^2} + \frac{8c_2' e^{-4} M^3}{\sqrt{\pi} r^3} - \frac{8c_2' e^{-4} M^4}{\sqrt{\pi} r^4} + \mathcal{O}(r^{-5}), \tag{51}$$

$$H(r) \approx c_1 + c_2 erf(2) + \frac{2c_2 e^{-4} M}{\sqrt{\pi} r} - \frac{4c_2 e^{-4} M^2}{\sqrt{\pi} r^2} + \frac{14c_2 e^{-4} M^3}{3\sqrt{\pi} r^3} - \frac{10c_2 e^{-4} M^4}{3\sqrt{\pi} r^4} + \mathcal{O}(r^{-5}). \tag{52}$$

As we know, for $\alpha \to 0$, the metric is expected to return to the Schwarzschild metric. To fulfill this desire, we must have: $c_1 = c_1' = c_2 = c_2' = 0$. To obtain the particular solution, we consider the following expansions

$$f_p(r) = \sum_{n=2} \frac{F_n}{r^n} = \frac{F_2}{r^2} + \frac{F_3}{r^3} ... \tag{53}$$

$$h_p(r) = \sum_{n=2} \frac{H_n}{r^n} = \frac{H_2}{r^2} + \frac{H_3}{r^3} ... \tag{54}$$

Inserting the above expansions into the field equations and solving order by order, one can get

$$f_p(r) = -\frac{1120\alpha M^3}{3r^7} - \frac{288\alpha M^4}{r^8} - \frac{756\alpha M^5}{r^9} - \frac{2016\alpha M^6}{r^{10}} - \frac{27216\alpha M^7}{5r^{11}} + \mathcal{O}\left(\frac{1}{r^{12}}\right) \tag{55}$$

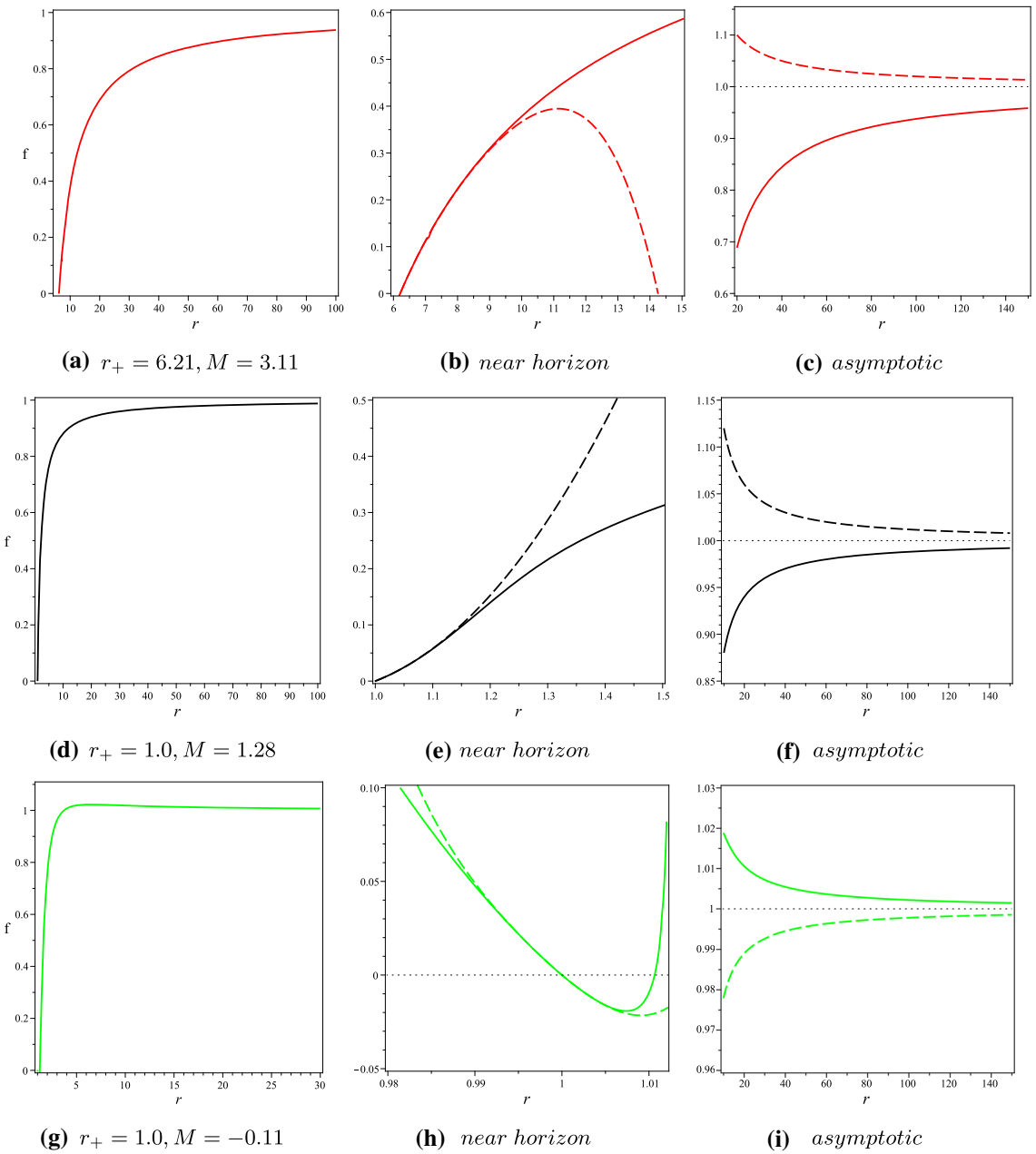

(a) $r_+ = 6.21, M = 3.11$ **(b)** *near horizon* **(c)** *asymptotic*

(d) $r_+ = 1.0, M = 1.28$ **(e)** *near horizon* **(f)** *asymptotic*

(g) $r_+ = 1.0, M = -0.11$ **(h)** *near horizon* **(i)** *asymptotic*

Fig. 8 The plots of metric for $c_1 = -0.25, \alpha = 0.5$

$$h_p(r) = -\frac{256\alpha M^3}{3r^7} - \frac{108\alpha M^4}{r^8} - \frac{252\alpha M^5}{r^9} - \frac{3024\alpha M^6}{5r^{10}} - \frac{81648\alpha M^7}{55r^{11}} + \mathcal{O}\left(\frac{1}{r^{12}}\right). \quad (56)$$

In large r, the solutions are:

$$f(r) \approx 1 - \frac{2M}{r} + f_p, \qquad h(r) \approx 1 - \frac{2M}{r} + h_p. \quad (57)$$

We wish to obtain an approximate analytic solution that is valid near the horizon and at large r. To this end we employ a continued fraction expansion, and write

$$h(r) = xA(x), \quad \frac{h(r)}{f(r)} = B^2(x), \quad (58)$$

with

$$A(x) = 1 - \epsilon(1-x) + (a_0 - \epsilon)(1-x)^2 + \tilde{A}(x)(1-x)^3 \quad (59)$$

$$B(x) = 1 + b_0(1-x) + \tilde{B}(x)(1-x)^2 \quad (60)$$

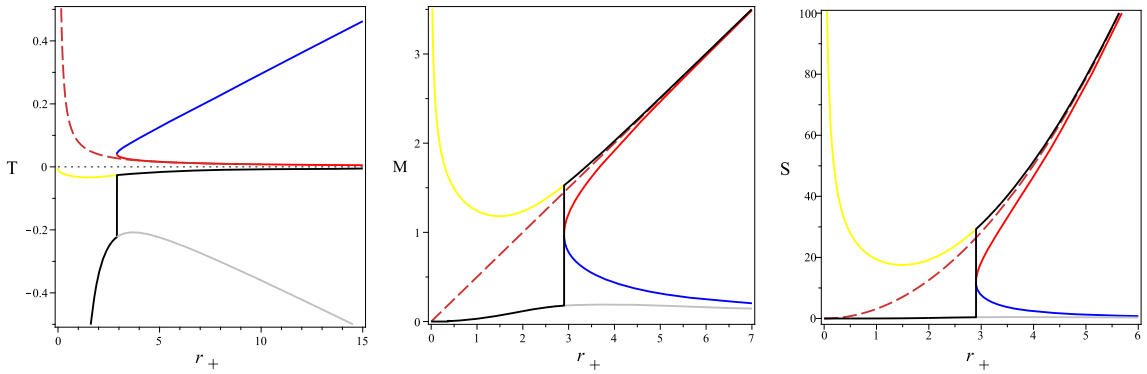

Fig. 9 The temperature, entropy and mass as a function of r_+ for $c_1 = \alpha = -0.5$. The orange dashed lines related to the Schwarzschild's black hole

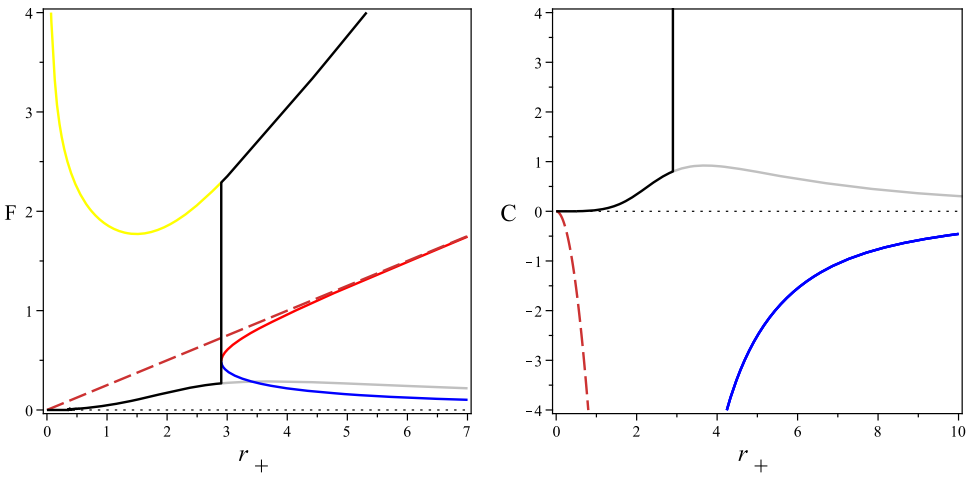

Fig. 10 The free energy and heat capacity as a function of r_+ for $c_1 = \alpha = -0.5$. The orange dashed lines related to the Schwarzschild's black hole

where

$$x = 1 - \frac{r_+}{r} \qquad \tilde{A}(x) = \cfrac{a_1}{1 + \cfrac{a_2 x}{1 + \cfrac{a_3 x}{1 + \cfrac{a_4 x}{1 + \ldots}}}}$$

$$\tilde{B}(x) = \cfrac{b_1}{1 + \cfrac{b_2 x}{1 + \cfrac{b_3 x}{1 + \cfrac{b_4 x}{1 + \ldots}}}} \tag{61}$$

where we truncate the continued fraction at order 4. By expanding (58) near the horizon ($x \to 0$) and the asymptotic region ($x \to 1$) we obtain

$$\epsilon = -\frac{H_1}{r_+} - 1, \qquad b_0 = \frac{F1 - H1}{2r_+}, \qquad a_0 = \frac{H_2}{r_+^2} \tag{62}$$

for the lowest order expansion coefficients, with the remaining a_i and b_i given in terms of (r_+, h_1, f_1, h_2); we provide these expressions in the Appendix. For a static space time we have a timelike Killing vector $\xi = \partial_t$ everywhere outside the horizon and so we obtain

$$T = \frac{1}{4\pi}\sqrt{\frac{f(r)}{h(r)}}h'(r)\bigg|_{r_+} = \frac{\sqrt{f_1 h_1}}{4\pi} = \frac{(1 - 2\epsilon + a_1 + a_0)}{4\pi r_+ (1 + b_1)}. \tag{63}$$

We compute the entropy by using of the first two term in continued fraction expansion as follows [33,34]

$$\begin{aligned} S &= -2\pi \int_{Horizon} d^2x \sqrt{\eta} \frac{\delta L}{\delta R_{abcd}} \epsilon_{ab}\epsilon_{cd} \\ &= \pi r_+^2 \left[1 + 6\alpha \left(\frac{2h_1}{r_+^3} - \frac{f_1 h_1}{r_+^2} + \frac{2h(r_+) f_1}{f(r_+) r_+^3} \right.\right. \\ &\quad \left.\left. + \frac{h(r_+) f_1^2}{f(r_+) r_+^2} + \frac{f(r_+) h_1^2}{h(r_+) r_+^2}\right)\right] \\ &= \pi r_+^2 \left[1 + 6\alpha \left(\frac{4h_1}{r_+^3} + \frac{f_1 h_1}{r_+^2}\right)\right]. \end{aligned} \tag{64}$$

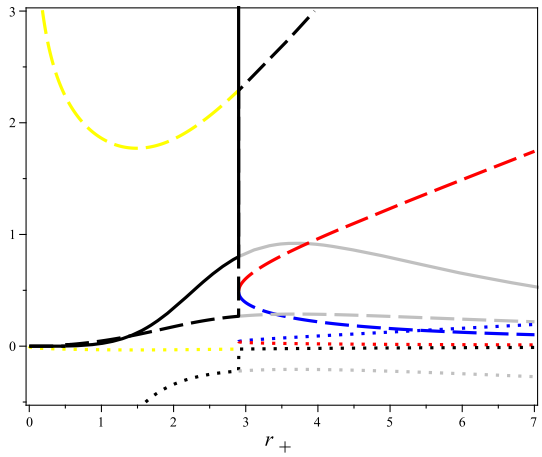

Fig. 11 The temperature (dotted line), heat capacity (solid line) and free energy (dashed line) as a function of r_+ for $c_1 = -0.25$, $\alpha = -0.5$

Then the mass from (25), becomes

$$M = \frac{\sqrt{f_1 h_1} r_+^2}{2}\left[1 + 6\alpha\left(\frac{4h_1}{r_+^3} + \frac{f_1 h_1}{r_+^2}\right)\right]. \tag{65}$$

To obtain the new black hole solutions we consider the different relations between f_1 and h_1 [35]. In the case of $f_1 = h_1$, we obtain the results of the first section.

3.1 The case $h_1 = f_1^3$

We now consider following relation between f_1 and h_1 as

$$h_1(r_+) = f_1^3(r_+). \tag{66}$$

From Eqs. (25) and (26), we have

$$M = \frac{f_1^2}{2r_+}(r_+^3 + 12\alpha r_+ f_1^4(r_+) + 48\alpha f_1^3(r_+)), \tag{67}$$

$$2r_+^4 f_1'(r_+) + 48\alpha r_+^2 f_1^4(r_+) f_1'(r_+) + 168\alpha r_+ f_1^3(r_+) f_1'(r_+) + f_1(r_+) r_+^3 - 24\alpha f_1^4(r_+) = 0. \tag{68}$$

Solving (68), one can achieve following equation as

$$\frac{1}{2} r_+^2 f_1^4 + \frac{24\alpha f_1^7}{r_+} + 6\alpha f_1^8 + c_1 = 0 \tag{69}$$

which leads to a maximum of eight solutions for $f_1(r_+)$ depending on the value of parameters. Inserting the solutions of (69) into the thermodynamical quantities, one can obtain the analytical solutions for them, which we have plotted in Figs. 9 and 10. In these figures, the dashed orange lines are the behavior of the thermodynamical quantities of Schwarzschild's black hole. In Fig. 9, the blue and red solid lines are the physical branches, because the temperatures and the mass of these branches are positive. Also, the red branch is globally and locally unstable and the blue branch is globally stable while locally unstable (Fig. 10). From the Fig. 11, there is a divergence in the heat capacity, but this divergence does not coincide with the extremum points of temperature and free energy. So, the phase transition does not occur.

In panels of Fig. 12, we have depicted the metric functions. In these figures, the mass of the black hole is positive and these solutions are similar to Schwarzschild's black hole.

4 Conclusion

In this paper, we studied the black hole solutions of Einsteinian cubic gravities by using continued fraction approximations. To get a complete solution, first, we constructed the near horizon and then asymptotic solutions and then used them to obtain an approximate analytic solution using a continued-fraction expansion. Then, we calculated the thermodynamic quantities like entropy, temperature and mass, and by inserting them in the first law and Smarr formula, we obtained the analytic solutions for the near horizon quantities. Then, one can obtain a metric according to continued fraction expansion that is only a function of constant integration not extra function like f_1 or h_1. We also showed that continued fraction expansion can be used to accurately approximate black hole solutions in cubic gravity, which are valid everywhere outside of the event horizon. Finally, to obtain the new black hole solutions, we considered the different relationships between the near horizon constants. We also compared our results with those of previous works on the subject and we found a good agreement between them. The important point in our work is that we assumed the near horizon constant f_1 in the first law of thermodynamic and the Smarr formula, is a function of the event horizon radius. This assumption is correct, because f_1 is proportional to temperature according to Eq. (23). This method is different from the one used in previous papers like [17,18]. First, they used the differential equations for metric function which have been obtained from the action of the theory, while, we have used the components of the field equations (3) of the theory. Second, they obtained the thermodynamical quantities from the first and the second term of near horizon expansion, while we obtained from the first law of thermodynamics and Smarr formula. Our method is applicable to every theory of gravity (as we previously applied to the quadratic gravity in reference [32]), while the method of the papers is only applicable for the theory in which the on-shell action is integrable with respect to r. Finally, this approach also allows us to obtain black hole solutions different from Einstein gravity solutions by assuming $f_1 \neq h_1$ in the near horizon expansion as we have done in Sect. 3. We think using the thermodynamics to obtain the black hole solutions is a normal approach with respect to one in the references [17,18].

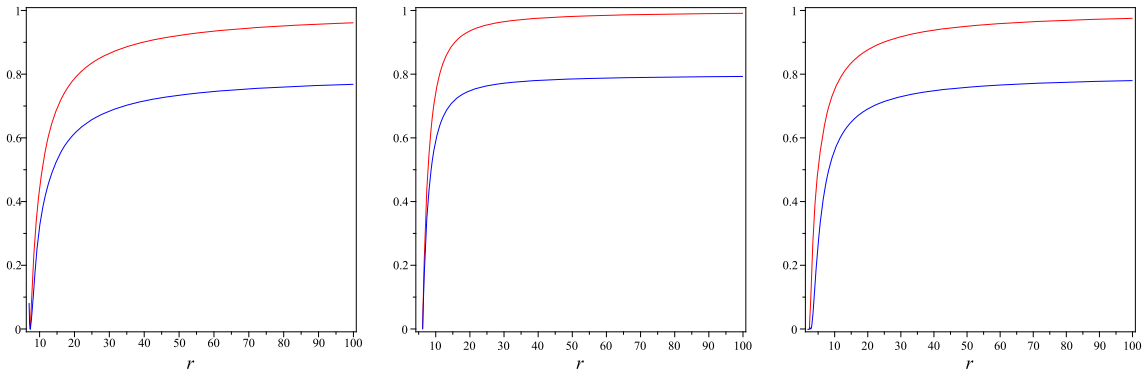

(a) $h_2 = 1, r_+ = 6$ **(b)** $h_2 = 2, r_+ = 6$ **(c)** $h_2 = 1, r_+ = 2$

Fig. 12 The behavior of $f(r)$ (blue line) and $0.8h(r)$ (red line) in terms of r for $c_1 = \alpha = -0.5$. Left: correspond to the red branch. Middle: correspond to the blue branch. Right: correspond to the yellow branch in Fig. 9

We leave for future work, obtaining the non-vacuum, rotating black hole, and other solutions of the theory by using the continued fraction expansion.

Appendix 1: Explicit terms in the continued fraction approximation

We present terms up to fourth order in the continued fraction approximation:

$$\epsilon = -\frac{F_1}{r_+} - 1, \quad a_1 = -1 - a_0 + 2\epsilon + r_+ f_1, a_2 = -\frac{4a_1 - 5\epsilon + 1 + 3a_0 + f_2 r_+^2}{a_1}$$
$$a_3 = -\frac{1}{a_1 a_2}\Big[- f_3 {r_+}^3 + a_1 {a_2}^2 + 5a_1 a_2 + 6a_0 + 10a_1 - 9\epsilon + 1\Big] \tag{70}$$
$$a_4 = -\frac{f_4 {r_+}^4 + a_1 {a_2}^3 + 2a_1 {a_2}^2 a_3 + a_1 a_2 {a_3}^2 + 6a_1 {a_2}^2 + 6a_1 a_2 a_3 + 15a_1 a_2 + 10a_0 + 20a_1 - 14\epsilon + 1}{a_1 a_2 a_3}$$

Acknowledgements The authors acknowledge the support of Shiraz University Research Council. We also thank the support of Iran National Science Foundation 99022223.

Data Availability Statement This manuscript has no associated data or the data will not be deposited. [Authors' comment: This study is a theoretical work, and there is no observational data.]

Funded by SCOAP[3]. SCOAP[3] supports the goals of the International Year of Basic Sciences for Sustainable Development.

Appendix B: Near horizon constants

Here, we present some near horizon constants regarding section (2) and (3) as follows:
The quantity f_4 is given in (8)

$$f_4 = \frac{-1}{3[{r_+}^{10}({r_+}^3 + 48\alpha f_1 + 24 r_+ \alpha {f_1}^2)(48 r_+ \alpha {f_1}^2 + 96\alpha f_1 + {r_+}^3)]}$$
$$\times \Big[- 31 {r_+}^{12} + 7524 {r_+}^{10} {f_1}^2 \alpha$$
$$- 11064 {r_+}^{11} {f_1}^3 \alpha - 4608 {r_+}^6 \alpha^2 {f_1}^2 - 86400 {r_+}^4 \alpha^3 {f_1}^4$$
$$+ 10944 {r_+}^7 {f_1}^3 \alpha^2 - 1534464 {r_+}^2 \alpha^4 {f_1}^6 +$$
$$888192 {r_+}^5 \alpha^3 {f_1}^5 - 89136 {r_+}^8 {f_1}^4 \alpha^2 - 5971968 \alpha^5 {f_1}^8$$
$$+ 5640192 \alpha^4 {f_1}^7 {r_+}^3 - 1769472 \alpha^3 {f_1}^6 {r_+}^6 +$$
$$184896 {r_+}^9 {f_1}^5 \alpha^2 + 1248 \alpha {r_+}^9 f_1 + 34 {r_+}^{13} f_1 - 864 \alpha {r_+}^8 \Big]. \tag{71}$$

The near horizon constants regarding Sect. (3):

$$f_3 = -\frac{1}{2592(f_1{}^3 h_1{}^2 r_+{}^2\alpha^2\left(r_+{}^3 f_1{}^3+8+6\,r_+{}^2 f_1{}^2+12\,r_+\,f_1\right))}$$
$$\times\Big[6912\alpha^2 f_1{}^6 h_2{}^2 r_+{}^4+71\,h_1{}^2 r_+{}^7 f_1{}^3-$$
$$160\,r_+{}^6 h_1{}^2 f_1{}^2+59\,r_+{}^5 h_1{}^2 f_1+30\,r_+{}^4 h_1{}^2$$
$$+5472\,\alpha^2 f_1{}^6 h_1{}^2 r_+{}^2$$
$$+4536\,\alpha^2 f_1{}^4 h_1{}^2+8892\,\alpha^2 f_1{}^5 h_1{}^2 r_+ +$$
$$876\,f_1{}^4 h_1{}^2 r_+{}^4\alpha+816\,f_1{}^5 h_1{}^2 r_+{}^5\alpha-792\,r_+{}^2 h_1{}^2\alpha\,f_1{}^2$$
$$+1728\,\alpha^2 f_1{}^7 h_1{}^2 r_+{}^3+6912\,\alpha^2 f_1{}^5 h_2{}^2 r_+{}^3-$$
$$816\,h_1 r_+{}^5 h_2 f_1{}^4\alpha+1728\,\alpha^2 f_1{}^7 h_2{}^2 r_+{}^5+684\,f_1{}^3 h_1{}^2 r_+{}^3\alpha$$
$$+576\,h_1 r_+{}^3 h_2 f_1{}^2\alpha-19584\,\alpha^2 f_1{}^5 h_1 r_+{}^2 h_2+$$
$$2496\,h_1 r_+{}^4 h_2 f_1{}^3\alpha-960\,h_1 r_+{}^6 f_1{}^5\alpha\,h_2-12384\,\alpha^2 f_1{}^6 h_1 r_+{}^3 h_2$$
$$-3456\,\alpha^2 f_1{}^7 h_1 r_+{}^4 h_2-17280\,\alpha^2 f_1{}^4 h_2 r_+\,h_1\Big]. \tag{72}$$

$$h_3 = -\frac{1}{2592(f_1{}^4 h_1 r_+{}^2\alpha^2\left(r_+{}^3 f_1{}^3+8+6\,r_+{}^2 f_1{}^2+12\,r_+\,f_1\right))}$$
$$\times\Big[11\,h_1{}^2 r_+{}^7 f_1{}^3-40\,r_+{}^6 h_1{}^2 f_1{}^2+35\,r_+{}^5 h_1{}^2 f_1$$
$$-6\,r_+{}^4 h_1{}^2+7200\,\alpha^2 f_1{}^6 h_1{}^2 r_+{}^2+8424\,\alpha^2 f_1{}^4 h_1{}^2$$
$$+12348\,\alpha^2 f_1{}^5 h_1{}^2 r_+ +948\,f_1{}^4 h_1{}^2 r_+{}^4\alpha+528\,f_1{}^5 h_1{}^2 r_+{}^5\alpha$$
$$-360\,r_+{}^2 h_1{}^2\alpha\,f_1{}^2+1728\,\alpha^2 f_1{}^7 h_1{}^2 r_+{}^3$$
$$+6912\,\alpha^2 f_1{}^5 h_2{}^2 r_+{}^3+6912\,\alpha^2 f_1{}^6 h_2{}^2 r_+{}^4+1728\,\alpha^2 f_1{}^7 h_2{}^2 r_+{}^5$$
$$+252\,f_1{}^3 h_1{}^2 r_+{}^3\alpha+576\,h_1 r_+{}^3 h_2 f_1{}^2\alpha-528\,h_1 r_+{}^5 h_2 f_1{}^4\alpha$$
$$+1920\,h_1 r_+{}^4 h_2 f_1{}^3\alpha-672\,h_1 r_+{}^6 f_1{}^5\alpha\,h_2-$$
$$14112\,\alpha^2 f_1{}^6 h_1 r_+{}^3 h_2-23040\,\alpha^2 f_1{}^5 h_1 r_+{}^2 h_2$$
$$-3456\,\alpha^2 f_1{}^7 h_1 r_+{}^4 h_2-17280\,\alpha^2 f_1{}^4 h_2 r_+\,h_1\Big]. \tag{73}$$

$$f_4 = \frac{-1}{248832(f_1{}^5 h_1{}^3 r_+{}^3\alpha^3\left(r_+{}^5 f_1{}^5+10\,r_+{}^4 f_1{}^4+80\,r_+{}^2 f_1{}^2+32+40\,r_+{}^3 f_1{}^3+80\,r_+\,f_1\right))}$$
$$\times\Big[-922\,h_1{}^3 r_+{}^7 f_1+2557\,h_1{}^3 r_+{}^{11} f_1{}^5+7713\,h_1{}^3 r_+{}^9 f_1{}^3-8528\,h_1{}^3 r_+{}^{10} f_1{}^4$$
$$-328\,h_1{}^3 r_+{}^8 f_1{}^2+813888\,\alpha^3 r_+{}^3 f_1{}^8 h_2 h_1{}^2-1990656\,\alpha^3 r_+{}^5 f_1{}^8 h_2{}^3+8136\,f_1{}^5 h_1{}^3 r_+{}^3\alpha^2$$
$$-59424\,f_1{}^4 h_1{}^3 r_+{}^6\alpha-1492992\,\alpha^3 r_+{}^7 f_1{}^{10} h_2{}^3+247896\,f_1{}^8 h_1{}^3 r_+{}^6\alpha^2+89712\,f_1{}^6 h_1{}^3 r_+{}^4\alpha^2$$
$$-248832\,\alpha^3 r_+{}^8 f_1{}^{11} h_2{}^3+143424\,f_1{}^9 h_1{}^3 r_+{}^7\alpha^2+384012\,f_1{}^7 h_1{}^3 r_+{}^5\alpha^2+230688\,\alpha^3 f_1{}^8 h_1{}^3 r_+{}^2$$
$$+248832\,\alpha^3 f_1{}^{10} h_1{}^3 r_+{}^4+316224\,\alpha^3 f_1{}^9 h_1{}^3 r_+{}^3+654480\,\alpha^3 f_1{}^7 h_1{}^3 r_++37164\,f_1{}^7 h_1{}^3 r_+{}^9\alpha$$
$$+31788\,f_1{}^3 h_1{}^3 r_+{}^5\alpha-15924\,f_1{}^6 h_1{}^3 r_+{}^8\alpha+4824\,r_+{}^4 h_1{}^3\alpha\,f_1{}^2$$
$$-6480\,r_+{}^2 h_1{}^3\alpha^2 f_1{}^4-7608\,h_1{}^3 r_+{}^7 f_1{}^5\alpha-2985984\,\alpha^3 r_+{}^6 f_1{}^9 h_2{}^3+124416\,\alpha^3 f_1{}^{11} h_1{}^3 r_+{}^5-$$
$$288000\,\alpha^2 r_+{}^6 f_1{}^7 h_2 h_1{}^2-492\,r_+{}^6 h_1{}^3+676512\,\alpha^3 f_1{}^6 h_1{}^3+237312\,\alpha^2 r_+{}^9 f_1{}^9 h_2{}^2 h_1-16128\,\alpha\,f_1{}^2 h_2 r_+{}^5 h_1{}^2$$
$$-829440\,\alpha^3 f_1{}^6 h_2{}^2 r_+{}^2 h_1-138240\,\alpha^2 f_1{}^4 h_2{}^2 r_+{}^4 h_1-399168\,\alpha^3 r_+{}^4 f_1{}^9 h_2 h_1{}^2-87024\,\alpha\,r_+{}^7 f_1{}^4 h_2 h_1{}^2+$$
$$1302912\,\alpha^3 r_+{}^2 f_1{}^7 h_2 h_1{}^2-356544\,\alpha^2 r_+{}^8 f_1{}^9 h_2 h_1{}^2$$
$$+580608\,\alpha^3 r_+{}^7 f_1{}^{11} h_2{}^2 h_1+2377728\,\alpha^3 r_+{}^3 f_1{}^7 h_2{}^2 h_1-414720\,\alpha^3 r_+{}^6 f_1{}^{11} h_2 h_1{}^2+2598912\,\alpha^3 r_+{}^6 f_1{}^{10} h_2{}^2 h_1$$
$$+4230144\,\alpha^3 r_+{}^5 f_1{}^9 h_2{}^2 h_1-460800\,\alpha^2 r_+{}^5 f_1{}^5 h_2{}^2 h_1-34560\,\alpha^2 r_+{}^7 f_1{}^7 h_2{}^2 h_1-1260288\,\alpha^2 r_+{}^6 f_1{}^6 h_2{}^2 h_1$$
$$+4105728\,\alpha^3 r_+{}^4 f_1{}^8 h_2{}^2 h_1+189360\,\alpha\,r_+{}^8 f_1{}^5 h_2 h_1{}^2+9072\,\alpha\,r_+{}^9 f_1{}^6 h_2 h_1{}^2-52128\,\alpha\,r_+{}^6 f_1{}^3 h_2 h_1{}^2$$
$$+110592\,\alpha^2 f_1{}^4 h_2 r_+{}^3 h_1{}^2-746496\,\alpha^3 f_1{}^6 h_2 r_+\,h_1{}^2-771264\,\alpha^2 r_+{}^7 f_1{}^8 h_2 h_1{}^2-50928\,\alpha\,r_+{}^{10} f_1{}^7 h_2 h_1{}^2$$
$$+313920\,\alpha^2 r_+{}^5 f_1{}^6 h_2 h_1{}^2-1022976\,\alpha^3 r_+{}^5 f_1{}^{10} h_2 h_1{}^2+1369728\,\alpha^2 r_+{}^4 f_1{}^5 h_2 h_1{}^2$$
$$+723456\,\alpha^2 r_+{}^8 f_1{}^8 h_2{}^2 h_1\Big]. \tag{74}$$

$$
\begin{aligned}
h_4 = & \frac{-1}{248832(f_1{}^6 h_1{}^2 r_+{}^3 \alpha^3 \left(r_+{}^5 f_1{}^5 + 10\, r_+{}^4 f_1{}^4 + 80\, r_+{}^2 f_1{}^2 + 32 + 40\, r_+{}^3 f_1{}^3 + 80\, r_+ f_1\right))} \\
& \times \Big[-810\, h_1{}^3 r_+{}^7 f_1 + 709\, h_1{}^3 r_+{}^{11} f_1{}^5 + 3177\, h_1{}^3 r_+{}^9 f_1{}^3 - 2832\, h_1{}^3 r_+{}^{10} f_1{}^4 \\
& - 424\, h_1{}^3 r_+{}^8 f_1{}^2 + 426816\, \alpha^3 r_+{}^3 f_1{}^8 h_2 h_1{}^2 - 1990656\, \alpha^3 r_+{}^5 f_1{}^8 h_2{}^3 - 251640\, f_1{}^5 h_1{}^3 r_+{}^3 \alpha^2 \\
& - 36576\, f_1{}^4 h_1{}^3 r_+{}^6 \alpha - 1492992\, \alpha^3 r_+{}^7 f_1{}^{10} h_2{}^3 + 354456\, f_1{}^8 h_1{}^3 r_+{}^6 \alpha^2 + 126576\, f_1{}^6 h_1{}^3 r_+{}^4 \alpha^2 \\
& - 248832\, \alpha^3 r_+{}^8 f_1{}^{11} h_2{}^3 + 129600\, f_1{}^9 h_1{}^3 r_+{}^7 \alpha^2 + 442476\, f_1{}^7 h_1{}^3 r_+{}^5 \alpha^2 - 377568\, \alpha^3 f_1{}^8 h_1{}^3 r_+{}^2 \\
& + 331776\, \alpha^3 f_1{}^{10} h_1{}^3 r_+{}^4 + 205632\, \alpha^3 f_1{}^9 h_1{}^3 r_+{}^3 - 482544\, \alpha^3 f_1{}^7 h_1{}^3 r_+ + 24780\, f_1{}^7 h_1{}^3 r_+{}^9 \alpha \\
& + 11532\, f_1{}^3 h_1{}^3 r_+{}^5 \alpha + 11628\, f_1{}^6 h_1{}^3 r_+{}^8 \alpha + 6552\, r_+{}^4 h_1{}^3 \alpha\, f_1{}^2 - 113616\, r_+{}^2 h_1{}^3 \alpha^2 f_1{}^4 - 26232\, h_1{}^3 r_+{}^7 f_1{}^5 \alpha \\
& - 2985984\, \alpha^3 r_+{}^6 f_1{}^9 h_2{}^3 + 124416\, \alpha^3 f_1{}^{11} h_1{}^3 r_+{}^5 - 472320\, \alpha^2 r_+{}^6 f_1{}^7 h_2 h_1{}^2 + 180\, r_+{}^6 h_1{}^3 + 116640\, \alpha^3 f_1{}^6 h_1{}^3 \\
& + 195840\, \alpha^2 r_+{}^9 f_1{}^9 h_2{}^2 h_1 - 11520\, \alpha\, f_1{}^2 h_2 r_+{}^5 h_1{}^2 - 829440\, \alpha^3 f_1{}^6 h_2{}^2 r_+{}^2 h_1 - 138240\, \alpha^2 f_1{}^4 h_2{}^2 r_+{}^4 h_1 \\
& - 1200960\, \alpha^3 r_+{}^4 f_1{}^9 h_2 h_1{}^2 - 54768\, \alpha\, r_+{}^7 f_1{}^4 h_2 h_1{}^2 + 1496448\, \alpha^3 r_+{}^2 f_1{}^7 h_2 h_1{}^2 - 301248\, \alpha^2 r_+{}^8 f_1{}^9 h_2 h_1{}^2 \\
& + 580608\, \alpha^3 r_+{}^7 f_1{}^{11} h_2{}^2 h_1 + 2377728\, \alpha^3 r_+{}^3 f_1{}^7 h_2{}^2 h_1 - 414720\, \alpha^3 r_+{}^6 f_1{}^{11} h_2 h_1{}^2 + 2847744\, \alpha^3 r_+{}^6 f_1{}^{10} h_2{}^2 h_1 \\
& + 5225472\, \alpha^3 r_+{}^5 f_1{}^9 h_2{}^2 h_1 - 460800\, \alpha^2 r_+{}^5 f_1{}^5 h_2{}^2 h_1 - 34560\, \alpha^2 r_+{}^7 f_1{}^7 h_2{}^2 h_1 - 1094400\, \alpha^2 r_+{}^6 f_1{}^6 h_2{}^2 h_1 \\
& + 5101056\, \alpha^3 r_+{}^4 f_1{}^8 h_2{}^2 h_1 + 124848\, \alpha\, r_+{}^8 f_1{}^5 h_2 h_1{}^2 + 8688\, \alpha\, r_+{}^9 f_1{}^6 h_2 h_1{}^2 - 43680\, \alpha\, r_+{}^6 f_1{}^3 h_2 h_1{}^2 \\
& + 276480\, \alpha^2 f_1{}^4 h_2 r_+{}^3 h_1{}^2 + 82944\, \alpha^3 f_1{}^6 h_2 r_+\, h_1{}^2 - 810432\, \alpha^2 r_+{}^7 f_1{}^8 h_2 h_1{}^2 - 31344\, \alpha\, r_+{}^{10} f_1{}^7 h_2 h_1{}^2 \\
& + 489024\, \alpha^2 r_+{}^5 f_1{}^6 h_2 h_1{}^2 - 1354752\, \alpha^3 r_+{}^5 f_1{}^{10} h_2 h_1{}^2 + 1342080\, \alpha^2 r_+{}^4 f_1{}^5 h_2 h_1{}^2 7 \quad + 599040\, \alpha^2 r_+{}^8 f_1{}^8 h_2{}^2 h_1 \Big].
\end{aligned}
\tag{75}
$$

Appendix C: Functions

Here, we present the functions regarding differential equations (45) and (46) as follows:

$$\gamma(r) = \frac{4r^7 - 9Mr^6 - 528\alpha M^2 r + 816\alpha M^3}{r(r-2M)(r^6 + 240\alpha M^2)}, \tag{76}$$

$$\eta(r) = \frac{2r^7 - 3Mr^6 - 528\alpha M^2 r + 1296\alpha M^3}{r(r-2M)(r^6 + 240\alpha M^2)}, \tag{77}$$

$$\omega(r) = \frac{2(2r^8 - 6Mr^7 + 3M^2 r^6 + 240\alpha M^2 r^2 - 1968\alpha M^3 r + 2736\alpha M^4)}{r^2(2M-r)^2(r^6 + 240\alpha M^2)}, \tag{78}$$

$$\Xi(r) = -\frac{2M(2r^7 - 5Mr^6 - 1008\alpha M^2 r + 1776\alpha M^3)}{r^2(r^6 + 240\alpha M^2)(2M-r)^2}, \tag{79}$$

$$g(r) = -\frac{1344\alpha M^3}{r^3(r^6 + 240\alpha M^2)}. \tag{80}$$

and

$$\bar{\gamma}(r) = \frac{2r^7 - 3Mr^6 - 352\alpha M^2 r + 864\alpha M^3}{r(r-2M)(r^6 + 160\alpha M^2)}, \tag{81}$$

$$\bar{\eta}(r) = \frac{2r^7 - 5Mr^6 - 352\alpha M^2 r + 544\alpha M^3}{r(r-2M)(r^6 + 160\alpha M^2)}, \tag{82}$$

$$\bar{\omega}(r) = \frac{2M^2(r^6 + 672r\alpha M - 1184\alpha M^2)}{r^2(r^6 + 160\alpha M^2)(2M-r)^2}, \tag{83}$$

$$\bar{\Xi}(r) = \frac{2(r^8 - 4Mr^7 + 3M^2 r^6 + 160\alpha M^2 r^2 - 1312\alpha M^3 r + 1824\alpha M^4)}{r^2(r^6 + 160\alpha M^2)(2M-r)^2}, \tag{84}$$

$$\bar{g}(r) = -\frac{896\alpha M^3}{r^3(r^6 + 160\alpha M^2)}. \tag{85}$$

References

1. T.P. Sotiriou, V. Faraoni, Rev. Mod. Phys. **82**, 451–497 (2010). https://doi.org/10.1103/RevModPhys.82.451. arXiv:0805.1726 [gr-qc]
2. T. Clifton, P.G. Ferreira, A. Padilla, C. Skordis, Phys. Rep. **513**, 1–189 (2012). https://doi.org/10.1016/j.physrep.2012.01.001. arXiv:1106.2476 [astro-ph.CO]
3. S. Nojiri, S.D. Odintsov, eConf **C0602061**, 06 (2006). https://doi.org/10.1142/S0219887807001928. arXiv:hep-th/0601213
4. S. Nojiri, S.D. Odintsov, Phys. Rep. **505**, 59–144 (2011). https://doi.org/10.1016/j.physrep.2011.04.001. arXiv:1011.0544 [gr-qc]
5. J.M. Maldacena, Adv. Theor. Math. Phys. **2**, 231–252 (1998). https://doi.org/10.1023/A:1026654312961. arXiv:hep-th/9711200
6. E. Witten, Adv. Theor. Math. Phys. **2**, 253–291 (1998). https://doi.org/10.4310/ATMP.1998.v2.n2.a2. arXiv:hep-th/9802150
7. D.M. Hofman, Nucl. Phys. B **823**, 174–194 (2009). https://doi.org/10.1016/j.nuclphysb.2009.08.001. arXiv:0907.1625 [hep-th]

8. M. Brigante, H. Liu, R.C. Myers, S. Shenker, S. Yaida, Phys. Rev. D **77**, 126006 (2008). https://doi.org/10.1103/PhysRevD.77.126006. arXiv:0712.0805 [hep-th]
9. J. de Boer, M. Kulaxizi, A. Parnachev, JHEP **03**, 087 (2010). https://doi.org/10.1007/JHEP03(2010)087. arXiv:0910.5347 [hep-th]
10. X.O. Camanho, J.D. Edelstein, JHEP **06**, 099 (2010). https://doi.org/10.1007/JHEP06(2010)099. arXiv:0912.1944 [hep-th]
11. K.S. Stelle, Phys. Rev. D **16**, 953 (1977). https://doi.org/10.1103/PhysRevD.16.953
12. R.C. Myers, B. Robinson, JHEP **08**, 067 (2010). https://doi.org/10.1007/JHEP08(2010)067. arXiv:1003.5357 [gr-qc]
13. J. Oliva, S. Ray, Class. Quantum Gravity **27**, 225002 (2010). https://doi.org/10.1088/0264-9381/27/22/225002. arXiv:1003.4773 [gr-qc]
14. A. Cisterna, N. Grandi, J. Oliva, Phys. Lett. B **805**, 135435 (2020). https://doi.org/10.1016/j.physletb.2020.135435. arXiv:1811.06523 [hep-th]
15. J. Ahmed, R.A. Hennigar, R.B. Mann, M. Mir, JHEP **05**, 134 (2017). https://doi.org/10.1007/JHEP05(2017)134. arXiv:1703.11007 [hep-th]
16. P. Bueno, P.A. Cano, Phys. Rev. D **94**(10), 104005 (2016). https://doi.org/10.1103/PhysRevD.94.104005. arXiv:1607.06463 [hep-th]
17. P. Bueno, P.A. Cano, Phys. Rev. D **94**(12), 124051 (2016). https://doi.org/10.1103/PhysRevD.94.124051
18. R.A. Hennigar, M.B.J. Poshteh, R.B. Mann, Phys. Rev. D **97**(6), 064041 (2018). https://doi.org/10.1103/PhysRevD.97.064041. arXiv:1801.03223 [gr-qc]
19. R.A. Hennigar, R.B. Mann, Phys. Rev. D **95**(6), 064055 (2017). https://doi.org/10.1103/PhysRevD.95.064055. arXiv:1610.06675 [hep-th]
20. M.B.J. Poshteh, R.B. Mann, Phys. Rev. D **99**(2), 024035 (2019). https://doi.org/10.1103/PhysRevD.99.024035. arXiv:1810.10657 [gr-qc]
21. A.M. Frassino, J.V. Rocha, Phys. Rev. D **102**(2), 024035 (2020). https://doi.org/10.1103/PhysRevD.102.024035. arXiv:2002.04071 [hep-th]
22. X.H. Feng, H. Huang, Z.F. Mai, H. Lu, Phys. Rev. D **96**(10), 104034 (2017). https://doi.org/10.1103/PhysRevD.96.104034. arXiv:1707.06308 [hep-th]
23. J. Jiang, B. Deng, Eur. Phys. J. C **79**(10), 832 (2019). https://doi.org/10.1140/epjc/s10052-019-7339-6
24. J.D. Edelstein, N. Grandi, A.R. Sánchez, JHEP **05**, 188 (2022). https://doi.org/10.1007/JHEP05(2022)188. arXiv:2202.05781 [hep-th]
25. P. Bueno, P.A. Cano, R.A. Hennigar, R.B. Mann, Phys. Rev. Lett. **122**(7), 071602 (2019). https://doi.org/10.1103/PhysRevLett.122.071602. arXiv:1808.02052 [hep-th]
26. P. Bueno, J. Camps, A.V. López, JHEP **04**, 145 (2021). https://doi.org/10.1007/JHEP04(2021)145. arXiv:2012.14033 [hep-th]
27. P. Bueno, P.A. Cano, A. Ruipérez, JHEP **03**, 150 (2018). https://doi.org/10.1007/JHEP03(2018)150. arXiv:1802.00018 [hep-th]
28. K. Kokkotas, R.A. Konoplya, A. Zhidenko, Phys. Rev. D **96**(6), 064007 (2017). https://doi.org/10.1103/PhysRevD.96.064007. arXiv:1705.09875 [gr-qc]
29. R.A. Konoplya, A.F. Zinhailo, Phys. Rev. D **99**(10), 104060 (2019). https://doi.org/10.1103/PhysRevD.99.104060. arXiv:1904.05341 [gr-qc]
30. A.F. Zinhailo, Eur. Phys. J. C **78**(12), 992 (2018). https://doi.org/10.1140/epjc/s10052-018-6467-8. arXiv:1809.03913 [gr-qc]
31. L. Rezzolla, A. Zhidenko, Phys. Rev. D **90**(8), 084009 (2014). https://doi.org/10.1103/PhysRevD.90.084009. arXiv:1407.3086 [gr-qc]
32. S.N. Sajadi, R.B. Mann, N. Riazi, S. Fakhry. https://doi.org/10.1103/PhysRevD.102.124026. arXiv:2010.15039 [gr-qc]
33. R.M. Wald, Phys. Rev. D **48**(8), R3427 (1993). https://doi.org/10.1103/PhysRevD.48.R3427. arXiv:gr-qc/9307038
34. V. Iyer, R.M. Wald, Phys. Rev. D **50**, 846 (1994). https://doi.org/10.1103/PhysRevD.50.846. arXiv:gr-qc/9403028
35. A. Bonanno, S. Silveravalle, Phys. Rev. D **99**(10), 101501 (2019). https://doi.org/10.1103/PhysRevD.99.101501. arXiv:1903.08759 [gr-qc]